Nummerical Optimization of Control of Multiple Carbon Qubits near a Nitrogen-Vacancy Center

Author

Tim Dikland

supervised by

Dr. Ir. T.H. Taminiau
Dr. N.V. Budko

Bachelor Thesis TU Delft

April, 2017

1 Abstract

The NV-center in diamond is a promising system for quantum information processing. The typical qubits are the electron spin in the NV-center and the surrounding ^{13}C nuclear spins. Fast and precise control of many ^{13}C spins is desirable but challenging due to crosstalk. Crosstalk is the unwanted effect of a control pulse on the other qubits. The coupled NV-^{13}C system is explored, and numerical techniques to optimize the control of multiple and single qubits are used. In this report the effect of the Bloch-Siegert shift in the weak driving regime is investigated first. This is done by studying the effect of a π-pulse when two carbon qubits are driven at the same time on resonance. It turns out that in this weak driving regime the effect of the off resonance is very small, and changes the fidelity not more than 0.3%. Furthermore the effect of a square π-pulse on 4 nearby qubits is studied. If the pulse is not optimized (thus square), the pulse cannot be done in less than $100\mu s$ while retaining at least 99% fidelity. By optimizing the envelope of the driving field using constrained optimization the pulse can be done in $22\mu s$ while retaining at least 99% fidelity.

2 Acknowledgements

Without extensive help, insight and encouragement it would have been impossible for me to complete this thesis. I would like to take a few words to express my appreciation to those who guided my through this project. First of all I would like to thank my supervisors Tim and Neil for their insight in the problem. Tim, thank you for your patience while introducing me in the wonderful world of quantum mechanics. It took me quite some time to get my head around the -sometimes hard to imagine- concepts. I am glad you never gave up trying to help me understanding the concepts. Neil, thank you for asking a question about every word you read. You really pushed me to the point that I became uncertain about what I actually knew, which helped me getting clearer what I wanted to say. Furthermore I would like to thank my family for supporting me and being there when I felt desperate for answers. Last but certainly not least I would like to thank my girlfriend, Esther. Thank you for making my life easier when I was busy, and thank you for helping me to create the images used in the report.

3 List of constants

Constants

Constant	Short description	value
D	Zero field splitting strength	$2\pi \times 2.878$ GHz
Q	Quaddrupolar splitting strength	$2\pi \times 4.946$ MHz
A^N	Hyperfine interaction strength electron Nitrogen	$2\pi \times 2.186$ MHz
γ_N	Gyromagnetic ratio nitrogen	$2\pi \times 3.077 \times 10^{-4}$ MHz/G
γ_e	Gyromagnetic ratio electron	$2\pi \times 2.802$ MHz/G
γ_C	Gyromagnetic ratio carbonspin	$2\pi \times 10.705 \times 10^{-4}$MHz/G

Experimental constants

Constant	Short description	value
$A^1_\perp$	Hyperfine interaction between NV centre and Carbon 1	$2\pi \times 55.0$ kHz
$A^1_\parallel$	Hyperfine interaction between NV centre and Carbon 1	$2\pi \times -11.0$ kHz
$A^2_\perp$	Hyperfine interaction between NV centre and Carbon 2	$2\pi \times 43.0$ kHz
$A^2_\parallel$	Hyperfine interaction between NV centre and Carbon 2	$2\pi \times 21.2$ kHz
$A^3_\perp$	Hyperfine interaction between NV centre and Carbon 3	$2\pi \times 26.0$ kHz
$A^3_\parallel$	Hyperfine interaction between NV centre and Carbon 3	$2\pi \times 24.7$ kHz
$A^4_\perp$	Hyperfine interaction between NV centre and Carbon 4	$2\pi \times 25.0$ kHz
$A^4_\parallel$	Hyperfine interaction between NV centre and Carbon 4	$2\pi \times -36.0$ kHz
$A^5_\perp$	Hyperfine interaction between NV centre and Carbon 5	$2\pi \times 12.0$ kHz
$A^5_\parallel$	Hyperfine interaction between NV centre and Carbon 5	$2\pi \times -48.7$ kHz

An overview of the (standard) matrices/operators used in this report

$$I_n = \begin{bmatrix} 1 & 0 & \cdots & 0 \\ 0 & 1 & & 0 \\ \vdots & & \ddots & \vdots \\ 0 & 0 & \cdots & 1 \end{bmatrix}$$ With n denoting the size of the (identity) matrix

$$S_x = \begin{bmatrix} 0 & 1 & 0 \\ 1 & 0 & 1 \\ 0 & 1 & 0 \end{bmatrix}$$

$$S_y = \begin{bmatrix} 0 & -i & 0 \\ i & 0 & -i \\ 0 & i & 0 \end{bmatrix}$$

$$S_z = \begin{bmatrix} 1 & 0 & 0 \\ 0 & 0 & 0 \\ 0 & 0 & -1 \end{bmatrix}$$

$$C_x = \begin{bmatrix} 0 & 1 \\ 1 & 0 \end{bmatrix}$$

$$C_y = \begin{bmatrix} 0 & -i \\ i & 0 \end{bmatrix}$$

$$C_z = \begin{bmatrix} 1 & 0 \\ 0 & -1 \end{bmatrix}$$

Contents

4 Introduction

One of the big challenges nowadays is to create a prototype of the quantum computer. The quantum computer in itself has a huge potential to solve important computational problems in polynomial time. The most important difference between a classical computer and the quantum computer is the qubit. Whereas the classical computer uses bits which can only be in one of two states, the qubits in the quantum computer can take on any superposition of two measurable states.
Although the advantages of the quantum computer are very clear there is still no working prototype today. This is because of some big technical difficulties in the way the quantum computer should be operated. One of them is that, unlike its classical counterpart, the quantum computer is very prone to disturbances in its states due to ambient energy. To reduce these effects experimental setups are cooled to low temperatures. Nevertheless the qubits still get corrupted. In order to detect if the state got corrupted a quantum error correction algorithm can be implemented.
Most quantum error correction algorithms require multiple qubits that are highly entangled. These algorithms would be speeded up if operations could be done on several qubits at the same time without undesired cross talk. A promising approach to this problem is to look at the nuclear spins of ^{13}C atoms near a NV center. Due to the interaction between the nuclear spins and the NV center, these nuclear spins are a good qubit candidate.
In this report a method of manipulating a qubit is derived. However, one can never prevent that nearby qubits are exposed to the control fields that were meant to manipulate another qubit. In order to avoid unwanted effects the control field is numerically optimized to avoid, cancel out, or minimize these effects. Therefore creating a fast and precise quantum operation. These optimized control fields could help to speed up processes in the quantum computer and thus could help to unleash the huge potential of the quantum computer

5 Theory

5.1 Nitrogen-vacancy centre

5.1.1 Molecular structure

A diamond consists of carbon atoms arranged in a cubical lattice. Imperfections in this crystal lattice are common. One of these imperfections is the so called nitrogen-vacancy centre (NV). This defect is the result of an impurity (a nitrogen atom) introduced during the growth of the diamond. One carbon atom will be substituted by a nitrogen atom, and one adjacent spot in the lattice will be left empty, the vacancy. Here we consider the negatively charged NV center, in which one extra electron is captured from the environment. A schematic view of the NV-centre can be found in figure 1.

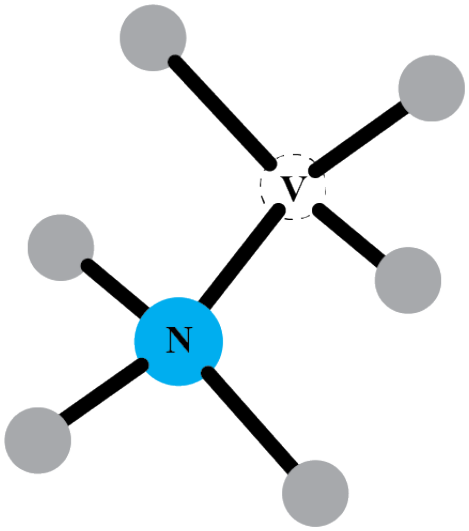

Figure 1: The NV-centre

In the setup used in this report the diamond is placed in a static magnetic field. The direction of the magnetic field is along the axis connecting the nitrogen to the vacancy.

5.1.2 Hamiltonian of the nitrogen-vacancy centre

It is necessery to know what the system Hamiltonian is. The Hamiltonian describes how the system evolves in time. Here the Hamiltonian consists of three parts. The first part describes the behaviour of the electron in the vacancy and its interaction with the static magnetic field. The second part describes the behaviour of the nitrogen atom and its interaction with the static magnetic field (B_z). The last part describes the interaction between the nitrogen atom and the electron in the vacancy. The system Hamiltonian is the sum of these

parts. Each of the parts is discussed in depth below.

The electron in the vacancy

The electronic spin of the NV center in the vacancy forms a $S = 1$ spin. This leads to it behaving like a spin triplet, with 2 distinct energies. They are separated by a zero field splitting of $D = 2\pi \times 2.878$ GHz. The electron also interacts with the static magnetic field. This interaction is better known as the Zeeman splitting. The strength of this interaction is determined by the gyromagnetic ratio of the electron of $\gamma_e = 2.802$ MHz/G. These effects combined yields part one of the system Hamiltonian (equation 1).

$$H_1/\hbar = DS_z^2 + \gamma_e B_z S_z \tag{1}$$

The nitrogen atom

The nitrogen atom considered in this report is a nitrogen-14 atom. This atom is also $S = 1$. The quadrupolar splitting is responsable for the splitting of the energy levels by $Q = 2\pi \times 4.946$ MHz. Here too the magnetic fields interacts with the nitrogen atom. The strength of this ineraction is again given by the gyromagnetic ratio of the ^{14}N atom, which is $\gamma_N = 2\pi \times 0.3077$ kHz/G. These effects combined yields part two of the system Hamiltonian (equation 2).

$$H_2/\hbar = QS_z^2 + \gamma_N B_z S_z \tag{2}$$

Hyperfine interaction

The last term of interest is the hyperfine interaction in the NV centre. The hyperfine interaction is given by $A_N = 2\pi \times 2.186$ MHz. In a later stage of this report a closer look is taken at the hyperfine interaction. Interested readers can skip to equation 8 and read from there. The third part of the Hamiltonian looks like equation 3.

$$H_3/\hbar = A_N S_z \otimes S_z \tag{3}$$

The system Hamiltonian

From this we can conclude the system Hamiltonian of the NV centre.

$$H = H_1 \otimes I_3 + I_3 \otimes H_2 + H_3 \tag{4}$$

$$H/\hbar = DS_z^2 \otimes I_3 + \gamma_e B_z S_z \otimes I_3 + I_3 \otimes QS_z^2 + I_3 \otimes \gamma_N B_z S_z + A_N S_z S_z \tag{5}$$

Or as physicists often like to put it shortly (writing S for the electron operators and I for the nitrogen operators. I is mathematically the same as the S)

$$H/\hbar = DS_z^2 + \gamma_e B_z S_z + QI_z^2 + \gamma_N B_z I_z + A_N S_z I_z \tag{6}$$

5.2 Carbon qubits

In the crystal lattice of diamond almost all of atoms are carbon atoms (aside from the impurities). Those carbon atoms are made up of ^{12}C (98.9%) which is spinless ($S = 0$) and ^{13}C (1.1%) which has spin ($S = 1/2$). Because the latter has $S = 1/2$ it interacts with (static) magnetic fields. Because the particle is a $S = 1/2$ particle, it has two distinctive eigenstates. Therefore they are a candidate for a qubit. From now on if carbon atoms or carbon qubits are mentioned, the ^{13}C atom is meant. In order to be a good qubit, it should be possible to manipulate the state of each qubit individually without altering the state of any other qubit. Right now, if we would place a few carbon qubits in empty space (with a static magnetic field along the z-axis), it would be quite impossible to change the state of one qubit without altering the other qubits. This problem is caused, because all the qubits have the same quantization axis and the energy levels are equal. Luckily the carbon qubits are not in empty space, but in a diamond lattice close to an NV centre. The interaction between the NV centre and the carbon qubit alters the eigenstates.

5.2.1 Hamiltonian of the carbon qubit

The interaction of the carbon atoms and a (static) magnetic field can be described by a Hamiltonian. Again the Zeeman effect is the one that governs the Hamiltonian. The strength of the interaction is given by the gyromagnetic ratio $\gamma_C = 2\pi \times 1.071$ kHz/G. The Hamiltonian is given in equation 7.

$$H/\hbar = \frac{1}{2}\gamma_C B_z C_z \tag{7}$$

Here C_i is the spin-i operator of the carbon qubit. The exact form of the operators can be found in the list of constants. From this equation can easily be seen that if only a static magnetic field is present all carbon qubits have the same Hamiltonian. Therefore they all have the same time evolution.

5.2.2 Hyperfine interaction

The interaction between the NV centre and the carbon qubits are hyperfine interactions. There are also interactions between the nitrogen atom and the carbon spin, and even interactions between two different carbon spins. However only the interaction between the electron and the carbon atom are considered. Because this interaction is much stronger because $\mu_e >> \mu_N, \mu_C$. Here μ is the magnetic moment which is defined as $\boldsymbol{\mu} = \gamma S$. Thus the other interactions can be safely omitted. The hyperfine interaction between the NV center and a carbon atom is given by equation 8.

$$H_{hf}/\hbar = \mu_e \mu_C \sum_{\mu,\nu=x,y,z} \left[\left(-\frac{8\pi}{3}|\psi(\mathbf{r}_C)|^2 + \left\langle \frac{1}{|\mathbf{r}_e - \mathbf{r}_C|^3} \right\rangle \right) \delta_{\mu,\nu} - 3 \left\langle \frac{n_\mu n_\nu}{|\mathbf{r}_e - \mathbf{r}_C|^3} \right\rangle \right] S_\mu \otimes C_\nu \tag{8}$$

Here the Fermi contact and the dipolar coupling are both included in this equation. Because in diamond the distance between the nuclear and the electron spin is relatively large, we can safely assume that $|\psi(\mathbf{r}_n)|^2 \approx 0$. Furthermore we can drop the average sign for the same reasoning. This simplifies equation 8 to

$$H_{hf}/\hbar = \mu_e \mu_C \sum_{\mu,\nu=x,y,z} \left[\frac{1}{|\mathbf{r}_e - \mathbf{r}_C|^3} \delta_{\mu,\nu} - 3 \frac{n_\mu n_\nu}{|\mathbf{r}_e - \mathbf{r}_C|^3} \right] S_\mu \otimes C_\nu \qquad (9)$$

In this equation $\delta_{\mu,\nu}$ is the Kronecker delta. n_i is a component of the unit vector $\mathbf{n}$ in the direction of $\mathbf{r} - \mathbf{r}_n$. μ_e is the magnetic moment of the electron and μ_C is the nuclear magnetic moment of the carbon atom. In the case that the magnetic field is relatively small, the zero field splitting is the largest energy involved. Since this energy is in the z-direction, the S_x and S_y terms (of the electron) in the Hamiltonian can be neglected. This approximation is called the secular approximation and is further explained in Appendix A. The hyperfine interaction can now be described by equation 10

$$H_{hf}/\hbar = \mu_e \mu_n \frac{1}{|\mathbf{r}_e - \mathbf{r}_C|^3} S_z \otimes [-3 n_z n_x C_x - 3 n_z n_y C_y + (1 - 3 n_z^2) C_z] \qquad (10)$$

This equation tells that the hyperfine interaction is only non-zero if the electron is in the $m_s = 1$ or $m_s = -1$ state. From now on we assume the NV-centre is placed in the $m_s = 1$, $m_N = 0$ state (m_N is the state of the nitrogen spin). It is later shown that the control pulses used will not disturb this configuration. A schematic impression of the system is given in figure 2

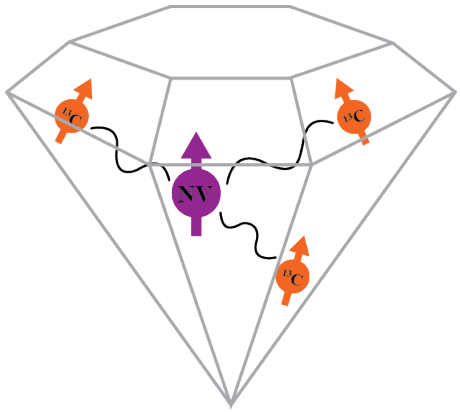

Figure 2: A schematic impression of a experimental setup with 3 carbon atoms

The effects of the hyperfine interaction can be captured in two components. The component parallel to the z-axis ($A_\parallel$) and the component perpendicular to the z-axis ($A_\perp$). These values have been measured in an existing NV-centre

and tabulated in the list of constants. The part of the Hamiltonian due to the hyperfine interaction can now be written in equation 11

$$H/\hbar = A_{\parallel} C_z + A_{\perp}(\cos(\theta) C_x + \sin(\theta) C_y) \tag{11}$$

Here θ is the angle in the x-y plane, measured from the positive x-axis to the positive y-axis. Therefore the total Hamiltonian for an (undriven) ^{13}C atom near a NV-centre can be written as

$$H/\hbar = (A_{\parallel} + \gamma_C B_z) C_z + A_{\perp}(\cos(\theta) C_x + \sin(\theta) C_y) \tag{12}$$

5.2.3 Spatial orientation

In this report it is supposed that all carbon atoms have $\theta = 0$ and thus lie in the x-z plane. It is now possible to define a new axis that is parallel with the eigenstates. This new axis is called z' and makes an angle ϕ with the original z-axis. In figure 3 it is made clear how this transformation works. The energy of the eigenstate is given by

$$P = \hbar \sqrt{(\gamma_C B_0 + A_{\parallel})^2 + A_{\perp}^2} \tag{13}$$

Now the Hamiltonian can be rewritten to

$$H_C/\hbar = P C_{z'} \tag{14}$$

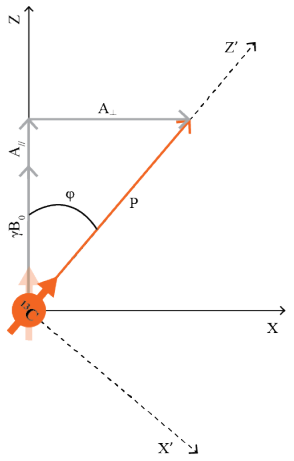

Figure 3: Transformation by rotating over an angle ϕ

5.3 Rabi oscillations

We observe the behaviour of a carbon two level system. The Hamiltonian is already derived in equation 14. The energies of the eigenstates are

$$\pm\hbar\sqrt{(\gamma B_0 + A_\parallel)^2 + A_\perp^2} \equiv \pm\hbar\epsilon \tag{15}$$

We now apply a magnetic driving field with frequency ω_d. The angle between the plane in which the magnetic field oscillates and the z'-axis we call ϕ. The strength of the driving field is much lower than ϵ in order to use the rotating wave approximation. The rotating wave approximation is further explained in appendix B. In order to simplify calculations and improve understanding the system is studied in a rotating frame (more information in appendix B), rotating with frequency ω_d. The Hamiltonian in the rotating frame (including the driving field) equals

$$H_{rot}/\hbar = (\epsilon - \omega_d + \gamma B_1 \sin(\phi)\cos(\omega_d t))C_z + \gamma B_1 \cos(\phi) C_x \tag{16}$$

The quantity $\epsilon - \omega_d$ is called the detuning (δ) and tells how far from resonance the driving field is. If $\phi = 0$ the problem can be easily solved analytically, and will give a good indication of how to use a driving magnetic field to manipulate the spin state of a carbon spin.

5.3.1 $\phi = 0$

If $\phi = 0$ the Hamiltonian loses its time dependence. The Hamiltonian is given by

$$H_{\phi=0}/\hbar = \delta C_z + \gamma B_1 C_x \tag{17}$$

The behaviour of a quantum state over time is always given by the Schrödinger equation.

$$i\hbar\frac{\partial}{\partial t}|\psi(t)\rangle = H|\psi(t)\rangle \tag{18}$$

In this time independent case the evolution is given by

$$|\psi(t)\rangle = \exp\left\{\frac{-i}{\hbar}H_{\phi=0}t\right\}|\psi(0)\rangle \tag{19}$$

We first look at an analytic derivation of the evolution of a arbitrary state $|\psi\rangle$. After that we show how to use the results in order to manipulate the state of single carbon spin. In order to evaluate the matrix exponential we have to diagonalize the matrix $\frac{-i}{\hbar}H_{\phi=0}t$. The eigenvalues of the Hamiltonian are given by $\mu_{\uparrow,\downarrow} = \pm\sqrt{\delta^2 + (\gamma B_1)^2}$. The up and down arrows indicate the positive or the negative value. Therefore the eigenvalues of the matrix we want to diagonalize are $\lambda_{\uparrow,\downarrow} = -it\mu_{\uparrow,\downarrow}$. The corresponding eigenvectors can be found by solving the corresponding linear equations.

$$\frac{-it}{\hbar}H_{\phi=0}\boldsymbol{v}_{\uparrow,\downarrow} = \lambda_{\uparrow,\downarrow}\boldsymbol{v}_{\uparrow,\downarrow} \tag{20}$$

We now solve this for $\boldsymbol{v}_\uparrow$. $\boldsymbol{v}_\downarrow$ can be calculated in the same fashion.

$$\boldsymbol{v}_\uparrow(2) = -\frac{(\delta - \mu_\uparrow)}{\gamma B_1}\boldsymbol{v}_\uparrow(1) \tag{21}$$

Here $\boldsymbol{v}_\uparrow(i)$ is written to denote the i^{th} component of the vector. Let $\sin(\theta) = \frac{\gamma B_1}{\mu_\uparrow}$, $\cos(\theta) = \frac{\delta}{\mu_\uparrow}$ and $\tan(\theta) = \frac{\gamma B_1}{\delta}$. We plug this in equation 21.

$$\boldsymbol{v}_\uparrow(2) = -\frac{(\delta - \mu_\uparrow)}{\gamma B_1}\boldsymbol{v}_\uparrow(1) \tag{22}$$

$$\boldsymbol{v}_\uparrow(2) = \left(\frac{\mu_\uparrow}{\gamma B_1} - \frac{\delta}{\gamma B_1}\right)\boldsymbol{v}_\uparrow(1) \tag{23}$$

$$\boldsymbol{v}_\uparrow(2) = \left(\frac{1}{\sin(\theta)} - \frac{1}{\tan(\theta)}\right)\boldsymbol{v}_\uparrow(1) \tag{24}$$

$$\boldsymbol{v}_\uparrow(2) = \tan\left(\frac{\theta}{2}\right)\boldsymbol{v}_\uparrow(1) \tag{25}$$

We now find the following eigenvectors.

$$\boldsymbol{v}_\uparrow = \begin{bmatrix}\cos\left(\frac{\theta}{2}\right)\\ \sin\left(\frac{\theta}{2}\right)\end{bmatrix} \quad \boldsymbol{v}_\downarrow = \begin{bmatrix}-\sin\left(\frac{\theta}{2}\right)\\ \cos\left(\frac{\theta}{2}\right)\end{bmatrix} \tag{26}$$

Since we have found the eigenvalues and respective eigenvalues we can now take the exponential of the matrix, and derive an expression for the evolution of the system ($\mu = \sqrt{\delta^2 + (\gamma B_1)^2}$).

$$\exp\left\{\frac{-iH_{\phi=0}t}{\hbar}\right\} = \exp\left\{\begin{bmatrix}\boldsymbol{v}_\uparrow & \boldsymbol{v}_\downarrow\end{bmatrix}\begin{bmatrix}\lambda_\uparrow & 0\\ 0 & \lambda_\downarrow\end{bmatrix}\begin{bmatrix}\boldsymbol{v}_\uparrow & \boldsymbol{v}_\downarrow\end{bmatrix}^{-1}\right\} \tag{27}$$

$$= \begin{bmatrix}\boldsymbol{v}_\uparrow & \boldsymbol{v}_\downarrow\end{bmatrix}\exp\left\{\begin{bmatrix}\lambda_\uparrow & 0\\ 0 & \lambda_\downarrow\end{bmatrix}\right\}\begin{bmatrix}\boldsymbol{v}_\uparrow & \boldsymbol{v}_\downarrow\end{bmatrix}^{-1} \tag{28}$$

$$= \begin{bmatrix}\boldsymbol{v}_\uparrow & \boldsymbol{v}_\downarrow\end{bmatrix}\begin{bmatrix}e^{\lambda_\uparrow} & 0\\ 0 & e^{\lambda_\downarrow}\end{bmatrix}\begin{bmatrix}\boldsymbol{v}_\uparrow & \boldsymbol{v}_\downarrow\end{bmatrix}^{-1} \tag{29}$$

$$= \begin{bmatrix}\cos(\mu t) + \frac{i\delta}{\mu}\sin(\mu t) & \frac{i\gamma B_1}{\mu}\sin(\mu t)\\ \frac{i\gamma B_1}{\mu}\sin(\mu t) & \cos(\mu t) - \frac{i\delta}{\mu}\sin(\mu t)\end{bmatrix} \tag{30}$$

Since we have found the analytic solution of the Schrödinger equation we can use this to manipulate a single carbon qubit. When this qubit is measured, there are two possible outcomes (the eigenstates). Either $m_C = 1/2 \rightarrow \begin{bmatrix}1\\0\end{bmatrix} \equiv |\uparrow\rangle$ or $m_C = -1/2 \rightarrow \begin{bmatrix}0\\1\end{bmatrix} \equiv |\downarrow\rangle$. Now say we know that the system is in one of its eigenstates at $t = 0$ (say the system is in the upstate). Then we know that $|\psi(0)\rangle = |\uparrow\rangle$. Now the evolution of this state is given by the Schrödinger

equation (equation 19). Since we have solved the equation we find:

$$|\psi(t)\rangle = \exp\left\{\frac{-i}{\hbar}H_{\phi=0}t\right\}|\uparrow\rangle = \begin{bmatrix}\cos(\mu t) + \frac{i\delta}{\mu}\sin(\mu t)\\ \frac{i\gamma B_1}{\mu}\sin(\mu t)\end{bmatrix} \tag{31}$$

From this we can calculate the probability of finding the up or down state after a certain amount of time.

$$P_{\uparrow\to\uparrow}(t) = |\langle\uparrow|\psi(t)\rangle|^2 = 1 - \frac{(\gamma B_1)^2}{\mu^2}\sin^2(\mu t) \tag{32}$$

$$P_{\uparrow\to\downarrow}(t) = |\langle\downarrow|\psi(t)\rangle|^2 = \frac{(\gamma B_1)^2}{\mu^2}\sin^2(\mu t) \tag{33}$$

A very useful quantum operation is the π-pulse. This is the operation that takes $|\uparrow\rangle$ to $|\downarrow\rangle$ and vice verse. We want this operation as precise and as quick as possible. For this system that means we want $\frac{\gamma B_1}{\mu}$ as close to one as possible. For that we need $\mu = \gamma B_1$ so that means $\delta = 0$ and that means $\omega_d = \epsilon$. In physical terms: we want the driving field on resonance. Thus if we choose $\omega_d = \epsilon$ we find the first maximum of equation 33 at $t = \frac{\pi}{2\mu}$. This is the typical pulse time, rewritten in equation 34

$$T = \frac{\pi}{2\sqrt{\delta^2 + (\cos(\phi)\gamma_C B_1)^2}} \tag{34}$$

If it happens to be that, for example due to technical limitations, the driving field is not exactly on resonance a good pulse can still be made by choosing $\gamma_C B_1 >> \delta$.

Example of single qubit control

In this section we use data of an existing NV-centre and carbon spin. Then we calculate the probabilities derived in the previous section. We also introduce a quantity to describe the closeness of two quantum states. This quantity is called the fidelity. The fidelity is defined as

$$F(\sigma, \rho) = tr\left[\sqrt{\sqrt{\rho}\sigma\sqrt{\rho}}\right]^2 \tag{35}$$

Here σ and ρ are density matrices. Since we are dealing with pure states, density matrices can be written as an outer product of a state with itself. Therefore we can say that $\sigma = |\phi\rangle\langle\phi|$ and $\rho = |\psi\rangle\langle\psi|$. If we now want to express the fidelity of two pure states, we can plug this into eq (35).

$$F(|\phi\rangle\langle\phi|, |\psi\rangle\langle\psi|) = |\langle\phi|\psi\rangle|^2 \tag{36}$$

Now we have all the tools to describe a existing system. The parameters used in this example will be summarized in table 1

B_0	B_1	ϕ	ω_d	$\|\psi(0)\rangle$
400G	1G	0	2.69 MHz	$\|\uparrow\rangle$

Table 1: Used constants and initial condition (example 1)

Using these values we find $\delta = 0$ and we expect our first flip (state $|\downarrow\rangle$) to happen at $t = \frac{\pi}{2\gamma B_1} = 234\mu s$. This is confirmed by the following figures. In figure 4 we see the fidelity between the state at time t and the down state. in figure 4 we also see the probability of measuring up or down as a function of the time. both figures run for $234\mu s$

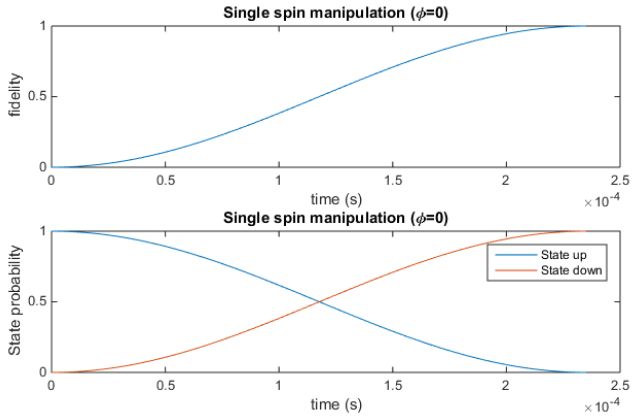

Figure 4: Fidelity of the π-pulse as function of time

5.3.2 $\phi \neq 0$

If $\phi \neq 0$ the Hamiltonian contains a time dependence. In this section we investigate the influence of this time dependence on the evolution of the system. First the Hamiltonian is investigated, to make an estimate of the effect. The Hamiltonian describing this problem should be written in terms of $C_{z'}$ and $C_{x'}$. Since the angle between the z-axis and the z'-axis is known ($= \phi = \arctan\left(\frac{A_\perp}{\gamma_C B_0 + A_\parallel}\right)$), we can write the Hamiltonian as

$$H_{\phi\neq 0}/\hbar = (\delta + \sin(\phi)\gamma_C B_1 \cos(\omega_d t))C_{z'} + \cos(\phi)\gamma_C B_1 C_{x'} \tag{37}$$

Now ω_d is chosen is such a way that $\delta = 0$. To see if the time dependant part has any effect on the evolution we first make a rough estimate. If we set $\cos(\omega_d t) = 1$ is the result is expected to be obviously worse than if we had not made this estimation. However, from the previous section it is clear that the fidelity of this evolution is

$$F_{max} = \frac{(\cos(\phi)\gamma_C B_1)^2}{(\sin(\phi)\gamma_C B_1)^2 + (\cos(\phi)\gamma_C B_1)^2} = \cos^2(\phi) \tag{38}$$

B_0	B_1	$A_\perp$	$A_\parallel$	ω_d	$\|\psi(0)\rangle$	Δt
400G	1G	55 kHz	-11 kHz	2.69 MHz	$\|\uparrow\rangle$	$10^{-10}s$

Table 2: used constants and initial condition (example 2)

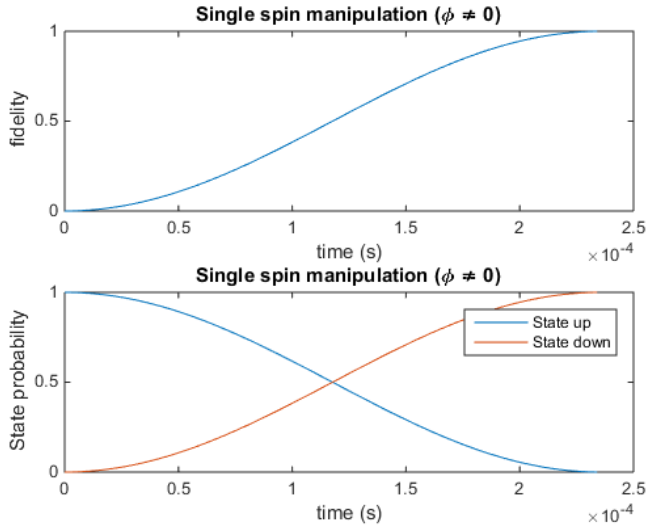

Figure 5: Fidelity of the pi-puls as function of time

If $\phi < 0.100$ rad, then the fidelity already is higher than 0.99. Since $\gamma_C B_0$ is much larger than the typical values of $A_\perp$ and $A_\parallel$ this is often the case. However it is plausible to assume that the effect is much smaller. In the slow driving limit ($\omega_d >> \gamma_C B_1$) $\cos(\omega_d t)$ changes sign very often. This leads to the expectation that the effect of this detuning averages to zero over the time of the pulse. To see the difference between using and omitting the time dependent term we simulate the evolution of a existing state using the backward Euler technique. The constants used are given in table 5.3.2. The backward Euler technique finds the next state using

$$|\psi(t+\Delta t)\rangle = -\left[H(t+\Delta t) - \frac{i\hbar}{\Delta t} I\right]^{-1} \frac{i\hbar}{\Delta t} |\psi(t)\rangle \tag{39}$$

Here I is the identity matrix with the same size as H. We can be sure that this technique is stable. Again the fidelity between $|\psi(t)\rangle$ and $|\downarrow\rangle$ is plotted together with the probability of finding the up and the down state. The figures again show a period of $234\mu s$

It looks like this figure is exactly the same as the one with $\phi = 0$. The maximum fidelity in this plot is 0.9999 so it we could have omitted the time-dependant term. From now on we assume the time-dependant oscillation in the detuning can be omitted if either the rotation of the atom is small or if the

driving strength is small.

5.3.3 Influence on the NV-center

As previously stated, the effect of the driving magnetic field (meant to change the carbon atoms state) on the NV-center itself is neglectable. Now we have also have some tools to reinforce that statement. The transition in the total system that is closest to that of a carbon spin, is the transition between $m_s = 1$, $m_N = 0$ to $m_s = 1$, $m_N = 1$. We can now estimate the probability that this transition is successfully driven with equation 33. If we take $\omega_d = 2.65$MHz and $A_N = 2\pi \times 2.186$MHz and take $B = 1$G for the driving field. The probability is estimated by

$$P_{NV,flip} = \frac{(\gamma_N B)^2}{(A_N - \omega_d)^2 + (\gamma_N B)^2} \approx 0 \tag{40}$$

So we don't have to worry about the state of the NV-centre changing during the calculations in this report.

5.4 Manipulating two ^{13}C spins simultaneously

5.4.1 Bloch-Siegert shift

In quantum computation it is beneficial to be able to control multiple qubits simultaneously. An analytical solution to the Schrödinger equation was derived in the previous section. One way to manipulate multiple qubits at the same time would be to calculate a control wave for the first carbon atom to flip in time T, and then calculate a control wave for the second atom to flip in time T. Now we send the superposition of both fields. Since the carbon qubits lie close to each other and the wavelength of the oscillating magnetic field is relatively big ($\lambda >> |r_1 - r_2|$), the magnetic field meant for carbon 1 will also be felt by atom 2 and vice versa. The effect of field 2 on carbon 1 can be approximated by the Bloch-Siegert shift. The Bloch-Siegert shift is an approximation how the off resonance field affects an carbon spin. If the driving pulse is not to strong ($\gamma B < \delta$), the effect of the off resonance field can be described as a small detuning. This detuning is what is called the Bloch-Siegert shift.

$$\delta_{BS} = \frac{(\gamma_C B_2)^2}{\omega_1 - \omega_2} \tag{41}$$

Here the index 2 is used to indicate the off-resonant field.

5.5 GRAPE

In this report numerical methods are used to find optimal parameters for several problems. All optimizations are performed to maximize a given fidelity. The methods in this report all depend on finding a good approximation for the gradient of the performance function (fidelity).

5.5.1 Discretized Hamiltonian

If the Hamiltonian has a time dependency that can not be omitted, one has to choose discrete time steps to estimate the Hamiltonian over a set interval. If a pulse take time T to complete, the interval is cut into N steps each of length $\Delta t = T/N$. When the simulation is actually performed a suitable number N is chosen. Within these time steps the Hamiltonian is assumed to be time-independant. The value of the Hamiltonian is $H(t_i)$ for the whole interval. Also the magnitude of the oscillating field is taken constant for that time interval. It is now possible to see that at each time interval there is a specific (constant) Hamiltonian. The Hamiltonian at a specific time interval is called a propagator. In this report the Hamiltonian is dependant on a magnetic field strength. This magnetic field strength is also discretized and taken constant in the time intervals. If there are multiple driving fields the field strength is contained in a vector $\boldsymbol{B}_j = \begin{bmatrix} B(1)_j \\ \vdots \\ B(n)_j \end{bmatrix}$ where $\boldsymbol{B}_j$ resembles the magnetic field of all n fields at time interval j. The propagator at time j looks like

$$U_j = \exp\{-i\Delta t H(t_j, \boldsymbol{B}_j)\} \tag{42}$$

In this report $H(t_j, \boldsymbol{B}_j)$ can be written as equation 43 for every problem. The Hamiltonian is made explicit in the chapter "Simulations and results".

$$H(t_j, \boldsymbol{B}_j) = \sum_{k=1}^{n} H_0 + B(k)_j H_{1,k} + B(k)_j^2 H_{2,k} \tag{43}$$

To calculate the evolution of a state during a pulse, the following relation is used

$$|\psi(t_j + \Delta t)\rangle = U_j |\psi(t_j)\rangle \tag{44}$$

5.5.2 Performance function

The function that is maximized is called the performance function. In this report the performance is described by the fidelity of the end state, so

$$\Phi = |\langle \psi_d | \psi_T \rangle|^2 \tag{45}$$

Here $|\psi_T\rangle = U_N \dots U_1 |\psi_0\rangle$ and $|\psi_d\rangle$ is the desired outcome. Now the gradient of this performance function is calculated. For more in depth derivation of these equation one could look in appendix C. In order to calculate the gradient of the performance function, the derivative of the propagator is calculated first. The derivative of the propagator is given by equation 46

$$\frac{\partial U_j}{\partial B(k)_j} = -i\Delta t(H_{1,k} + 2B(k)_j H_{2,k}) U_j \tag{46}$$

Now it is possible to calculate the gradient of the performance function

$$\frac{\partial \Phi}{\partial B(k)_j} = 2\,\mathrm{Re}(\langle \psi_d | -i\lambda_j \Delta t (H_{1,k} + 2B(k)_j H_{2,k}) \psi_j \rangle \langle \psi_T | \psi_d \rangle) \tag{47}$$

with $\lambda_j = U_N \cdots U_{j+1}$

5.5.3 Pulse Engineering

If the performance function (Φ) and its gradient ($\nabla\Phi$) are known, it is possible to use GRAPE to engineer an optimal pulse. A general outline of the algorithm is stated below.

- **Step 1)** Define a stepsize ϵ that dictates the maximal change in the parameters
- **Step 2)** Calculate the gradient of the performance function
- **Step 3)** Update the vector with paramaters ($\boldsymbol{B}$) according to $\boldsymbol{B}_{new} = \boldsymbol{B}_{old} + \epsilon\nabla\Phi$
- **Step 4)** Repeat step 1 to 3 for M times
- **Step 5)** Calculate the value of the performance function and return the value of the performance function and the optimized parameter vector $\boldsymbol{B}$

The choice of ϵ is important in this algorithm, since it determines the performance of the algorithm. If ϵ is large the algorithm can overshoot the optimum and therefore may not find good results. If ϵ is small the chance of finding a good result is better, but the convergence of the algorithm can be very slow. Because the next section is basically an enhancement of GRAPE, it is not used to create do simulations in this report.

5.6 Constrained Optimization

If the the performance function (Φ) and its gradient ($\nabla\Phi$) are known, it is also possible to use other algorithms to find an optimal solutions. One of the flaws of GRAPE as it is defined above, is that it is impossible to set bounds for the values of $\boldsymbol{B}$. The Matlab toolbox constrained optimization allows such bounds. Also the optimization algorithms tend to converge faster and closer to an optimum. It is possible to use the derivative calculated for the GRAPE algorithm as an explicit input for the constrained optimization algorithms.

5.6.1 the constrained optimization algorithm

The constrained optimization algorithm tries to minimize a function $f(\boldsymbol{b})$ in such a way that the parameters are within a set range.

$$\min_b f(b) \quad \text{such that} \quad lb < b(i) < ub \quad \text{for all i} \tag{48}$$

Here lb is the lower bound of the variable and ub is the upper bound of the variable. An algorithm that handles this problem fast and accurately is the interior point algorithm. This algorithm uses a logarithmic barrier function in order to not converge to a value out of bounds. Another advantage of using this algorithm is that the performance stays good if the problem becomes more complex. This might be useful in further research. A detailed explanation of the algorithm can be found in [5]. The number of time intervals (N) is chosen in such a way that the solution does not change significantly anymore.

6 Simulation and results

In this chapter, two different experiments are investigated. The first one takes a closer look at the effect of the Bloch-Siegert shift in weakly driven carbon atoms. After that we try to use GRAPE and constrained optimization methods to explore the options of calculating a better pulse. The second experiment tries to find an (optimal) pulse to do a π-pulse on exactly one out of 5 carbon atoms. For these simulations the parameters of an existing NV center are used. These are tabulated in the list of constants.

6.1 Bloch-Siegert shift in weakly driven qubits

The first simulation experiments looks at the effect of the Bloch-Siegert shift in the weak driving regime. A superposition of two magnetic fields, each on resonance with one of the two qubits, is send to the system. In the weak driving regime the strength of the magnetic driving field is so small that $30\gamma_C B_i \approx \delta$. In this regime the Bloch-Siegert shift is the only significant effect of the off resonance field, and the Hamiltonian van be written as

$$H_{weakBS} = H_{C1} \otimes I_2 + I_2 \otimes H_{C2} \tag{49}$$

In this equation H_{C1} and H_{C2} are given by

$$H_{C1}/\hbar = \left[\cos(\phi)\frac{(\gamma B_2)^2}{2(\omega_1 - \omega_2)}\right] C_z + \cos(\phi) B_1 \gamma C_x \tag{50}$$

$$H_{C2}/\hbar = \left[\cos(\phi)\frac{(\gamma B_1)^2}{2(\omega_2 - \omega_1)}\right] C_z + \cos(\phi) B_2 \gamma C_x \tag{51}$$

First we test how the (non-optimized) block wave works. As an example we use qubit 1 and 2 from the list of constants. To this end we set the magnetic field strength for the field resonant with qubit 1 to a range of values between 3δ and 30δ. Then we calculate the pulse time with equation 34. Next the driving strength of field 2 is calculated in order to give it the same pulse time. the results are plotted in figures 6

Two things are apparent from this figure. The first thing is that the fidelity tends to increase as the pulse time becomes longer. This was an expected effect. The spatial orientation of both spins forces the amplitude of the magnetic field to be roughly the same. Therefore the driving effect (order 1 in Hamiltonian) becomes more and more dominant over the Bloch-Siegert shift (order 2 in Hamiltonian) the longer the pulse time becomes. The second thing that can be seen in the figure is that even though the Bloch-Siegert shift has an effect (if it did not have an effect, the fidelity would be one for all pulse times) the effect is not that big. Even at the lowest pulse times possible in this driving regime, the overall fidelity stays above 99% with margin.

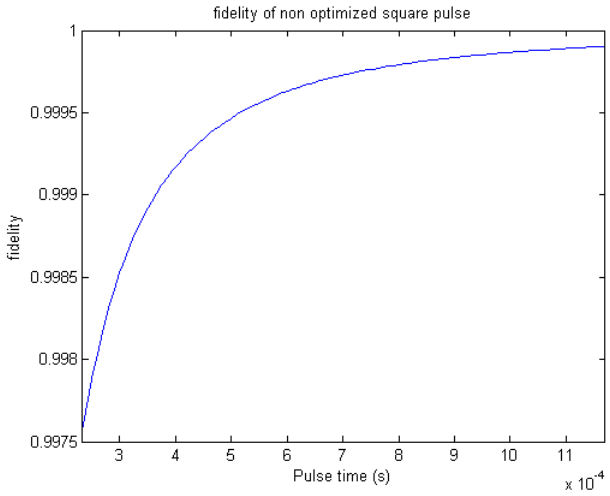

Figure 6: The fidelity of the naive square pulse for different pulse times

6.2 Improved π-pulse

In this section a π-pulse on one qubit is engineered, while leaving up to 4 other states untouched. This π-pulse is being driven by a magnetic field with one frequency. This frequency is chosen on resonance with the qubit we want to flip. It is important to look at the system Hamiltonian first. The system Hamiltonian looks like

$$H_{oneflip} = H_{C1}\otimes I_{16}+I_2\otimes H_{C2}\otimes I_8+I_4\otimes H_{C3}\otimes I_4+I_8\otimes H_{C4}\otimes I_2+I_{16}\otimes H_{C5} \quad (52)$$

With for each H_{C_i}

$$H_{C_i} = \delta_i C_z + \cos(\phi_i)\gamma_C B_1 C_x \quad (53)$$

6.3 Square pulses (Rabi)

First we calculate a square pulse amplitude to flip to the desired state as if the other carbon atoms were not there. From the Rabi equation (equation 33) a high fidelity is expected when the time is very long (and thus the magnetic field weak). It is also expected that the fidelity goes down as the time for the pulse becomes shorter. To see how the fidelity deteriorates as the field becomes stronger, the flipping probabilities are plotted for increasingly smaller T (and thus increasingly higher B). The time T is divided by two every next figure. The results can be seen in figure 7
From the figure can be seen that the first qubit always is flipped at the end. This is exactly what was expected, since the magnetic field and time where chosen in such a way that would be exactly flipped at the end. However, if the pulse time becomes smaller there is a significant chance some other states would have

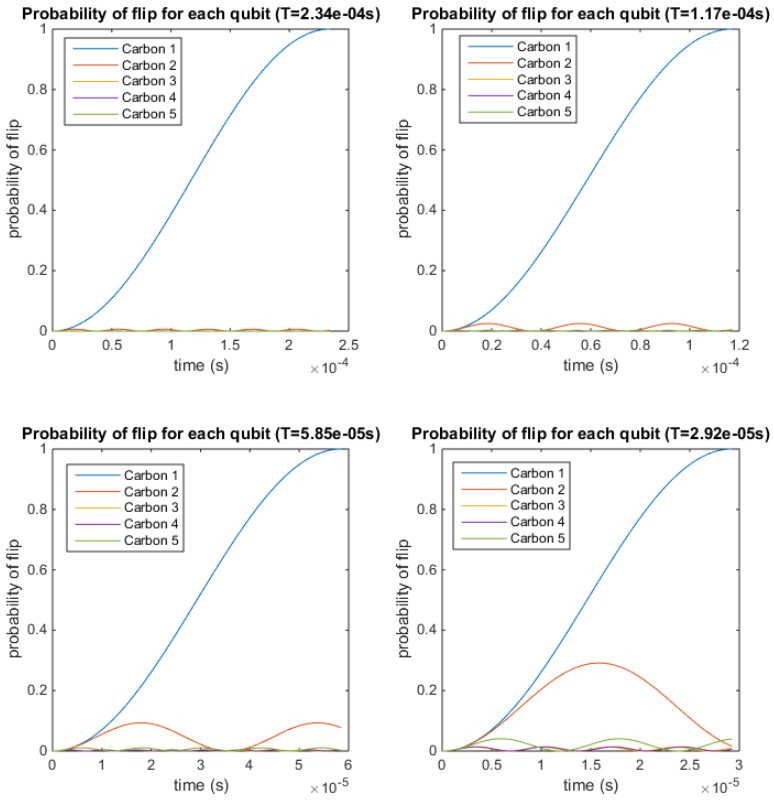

Figure 7: Flipping probablities for each qubit. The pulse time is halved between each figure.

flipped too. This simulation is made for a lot of different times and the results can be seen in figure 8.
Since a fidelity of $> 0.99\%$ is considered good, and anything below as bad, it looks like a good idea to start looking for optimal pulses in the region $10\ \mu s < T < 90\ \mu s$. In this region the square wave solution starts giving unacceptable results. We do this the constrained optimization method. In the method of constrained optimization we use $B_{max} = 2B_{ref}$, where B_{ref} is the amplitude of the square pulse.

6.3.1 Constrained optimization

With the method of constrained optimization the shortest pulse with an fidelity higher than 99% was $22\mu s$ long. The amplitudes of the optimal pulse are given

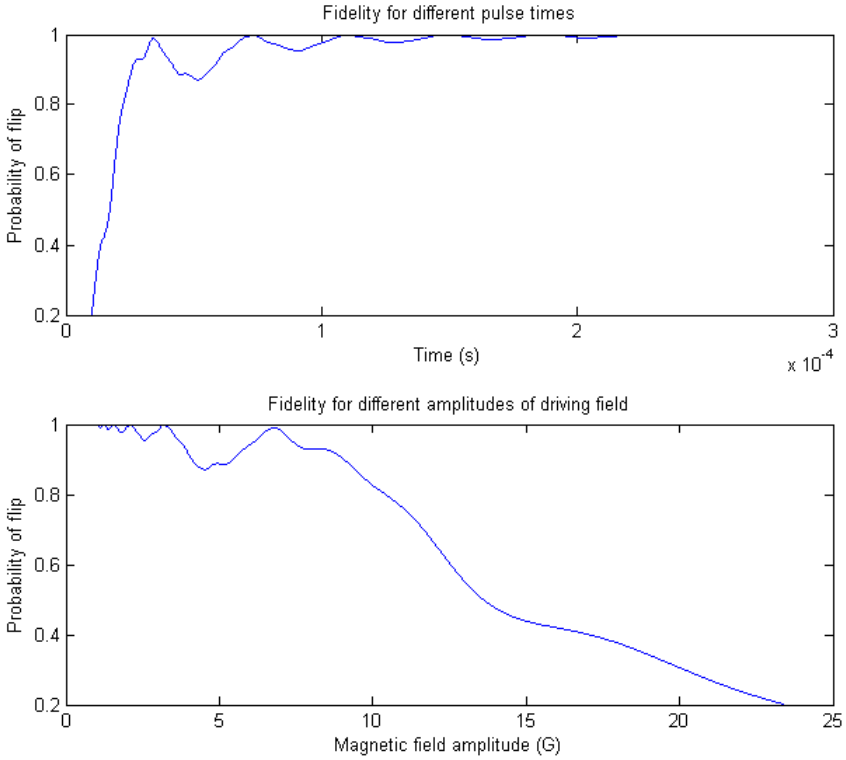

Figure 8: Fidelity for different square pulses

in figure 9
If that pulse is done on the system, we can again look what the probability of flipping of each individual qubit in time is. Those probabilities are plotted in figure 10.

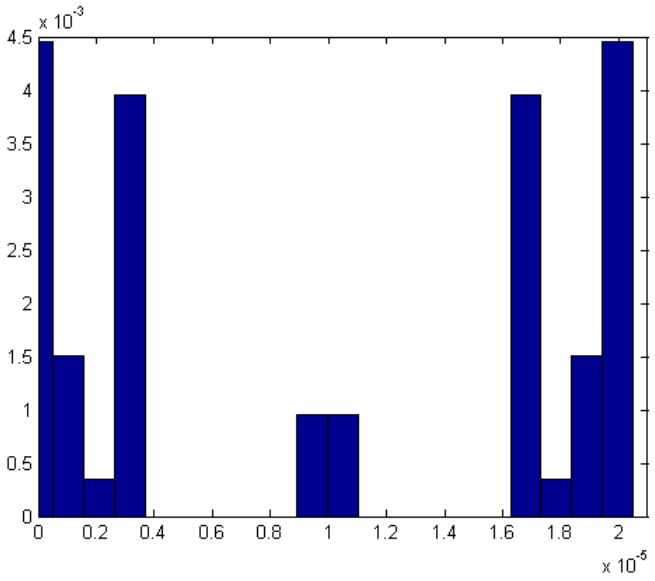

Figure 9: Optimal amplitudes for a π-pulse in $22\mu s$

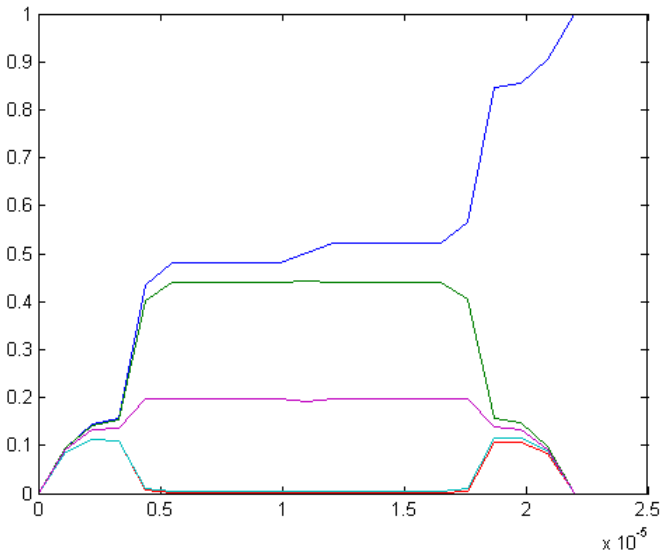

Figure 10: flipping probabilities for an optimal π-pulse in $22\mu s$

.

7 Conclusion and discussion

7.1 Conclusion of simulations

From the simulations performed in the previous chapter some things have become clear. The first conclusion is that in the weak driving regime ($30\gamma_C B < \delta$) when driving two qubits simultaneously with same order fields, the impact of the Bloch-Siegert shift is rather small. For further calculations in this regime the effect of the Bloch-Siegert shift can be neglected. Therefore two carbon spins can be driven at the simultaneously in this regime. The second conclusion is that it is possible to generate a nearly perfect π-puls on one qubit (and leaving the other states unchanged) in the driving regime where the simple square pulses no longer give good results.

7.2 Recommendations for further research

In this report we only covered a small regime where the Bloch-Siegert shift happens. In further research other regimes can be investigated and a new Hamiltonian can then be optimized. Furthermore we only looked at the amplitude of the magnetic control field. In further research one could also take the phase of the control field into account, and try to use this parameter in optimization routines in order to further enhance control fields.

References

[1] A. Reiserer, N. Kalb et al. *Robust quantum-network memory using decoherence-protected subspaces of nuclear spins.*, 2016

[2] H. Bernien. *Control, Measurement and entanglement of remote quantum spin registers in diamond*, 2014

[3] C.P. Slichter. *Principles of Magnetic Resonance*, 1990, Springer

[4] M. Ijspeert. *Numerical Optimization of Microwave and Radio Frequency Control Pulses for the Nitrogen-Vacancy Electron-Nuclear Spin Register*, 2015

[5] S.J. Wright. *Primal-Dual Interior-Point Methods*, 1997, SIAM

Appendices

Appendix A: Rotating wave approximation

The rotating wave approximation is made to, together with a rotating frame, turn a linearly polarized oscillating magnetic field into a static magnetic field in the rotating frame. At the hart of the approximation lies the fact that a linearly polarized magnetic field with frequency ω can be written as the superposition of two circularly polarized fields with frequency ω and $-\omega$. In the case that ω is chosen in such a way that it is very close to the splitting energy of two eigenstates. That way the rotating wave approximation can be useful. The field with frequency ω is said to be on resonance and will be dominant. The field with frequency $-\omega$ is off resonance. If the driving of the field is not to strong the off resonance field will average to zero fairly quickly. The rotating wave approximation tells us we can omit these off resonance terms.

Appendix B: Secular approximation

The secular approximation is made if the energy splitting (due to hyperfine interaction) in one direction is much smaller than in any other orthogonal direction. The influence on the eigenvalues of the Hamiltonian by these smaller energies can be neglected because they are only a second order effect. A simple example is given below. Suppose a hypothetical system with Hamiltonian

$$H = aS_z \otimes I_2 + bS_z \otimes C_z + cS_x \otimes C_z$$

With $a >> b, c$. The eigenvalues of this Hamiltonian (which define the energy splittings) are 0, 0, $\sqrt{(a+b)^2 + c^2}$, $\sqrt{(a-b)^2 + c^2}$, $\sqrt{(a+b)^2 - c^2}$ and $\sqrt{(a-b)^2 - c^2}$. We use the Laurent series of $\sqrt{x^2 + a}$ to approximate these eigenvalues. $\sqrt{x^2 + a} = \sum_0^\infty \frac{(-1)^n (2n)! a^n}{(1-2n)n!^2 4^n x^{2n-1}} = x + \frac{a}{2x} - \mathcal{O}(x^{-2})$ If In this case $x >> a$ we can approximate this root by $\sqrt{x^2 + a} \approx x$. In this example $a >> b, c$ so we could approximate the eigenvalues by 0, 0, $a + b$, $a - b$, $-a - b$, $-a + b$. The same could be done for all $S_{x,y,z} \otimes I_{x,y,z}$. The general result is: if the leading term $aS_z \otimes_2$ is large enough only the terms containing S_z are of importance. This is what we call the secular approximation.

Appendix C: Derivation of GRAPE components

The derivation of $\frac{\partial U_j}{\partial B(k)_j}$ can be found below. Here a result from matrix analysis is used. This result is written down below

$$\frac{d}{dt}e^{X(t)} = \int_0^1 e^{\alpha X(t)} \frac{X(t)}{dt} e^{(1-\alpha)X(t)} d\alpha \tag{54}$$

If we now can write the Hamiltonian at time $t = t_j$ as

$$H(t_j, \boldsymbol{B}_j) = \sum_{k=1}^{n} H_0 + B(k)_j H_{1,k} + B(k)_j^2 H_{2,k} \tag{55}$$

For the readability of the proof we write H_j for $\sum_{k=1}^{n} H_0 + B(k)_j H_{1,k} + B(k)_j^2 H_{2,k}$. Also the change of variables $\Delta t d\alpha = d\tau$ is made in the proof.

$$\frac{\partial U_j}{\partial B(k)_j} = \frac{\partial}{B(k)_j} e^{-i\Delta t H_j} \tag{56}$$

$$= \int_0^1 e^{\alpha(-i\Delta t H_j)} \frac{d(-i\Delta t H_j)}{dB(k)_j} e^{(1-\alpha)(-i\Delta t H_j)} d\alpha \tag{57}$$

$$= \int_0^1 e^{\alpha(-i\Delta t H_j)} (-i\Delta t) \frac{dH_j}{dB(k)_j} e^{(1-\alpha)(-i\Delta t H_j)} d\alpha \tag{58}$$

$$= \int_0^{\Delta t} e^{(-i\tau H_j)} (-i \frac{dH_j}{dB(k)_j}) e^{i(\tau - \Delta t)H_j} d\tau \tag{59}$$

$$= -i \int_0^{\Delta t} e^{-i\tau H_j} \frac{dH_j}{dB(k)_j} e^{i\tau H_j} d\tau \cdot e^{-i\Delta t H_j} \tag{60}$$

$$= -i \int_0^{\Delta t} e^{-i\tau H_j} \frac{dH_j}{dB(k)_j} e^{i\tau H_j} d\tau \cdot U_j \tag{61}$$

$$= -i \int_0^{\Delta t} (I - i\tau H_j + \mathcal{O}(\tau^2)) \frac{dH_j}{dB(k)_j} (I + i\tau H_j + \mathcal{O}(\tau^2)) d\tau \cdot U_j \tag{62}$$

$$= -i \int_0^{\Delta t} (\frac{dH_j}{dB(k)_j} + i\tau [\frac{dH_j}{dB(k)_j} H_j - H \frac{dH_j}{dB(k)_j}] + \mathcal{O}(\tau^2)) d\tau \cdot U_j \tag{63}$$

$$= -i \int_0^{\Delta t} (\frac{dH_j}{dB(k)_j} + \mathcal{O}(\tau)) d\tau \cdot U_j \tag{64}$$

$$= -i\Delta t \frac{dH_j}{dB(k)_j} U_j + \mathcal{O}(\Delta t^2) \tag{65}$$

$$= -i\Delta t (H_{1,k} + 2B(k)_j H_{2,k}) U_j + \mathcal{O}(\Delta t^2) \tag{66}$$

The derivation of $\frac{\partial \Phi}{\partial B(k)_j}$ can be found below.

$$\frac{\partial \Phi}{\partial B(k)_j} = \frac{\partial}{\partial B(k)_j} |\langle \psi_d | \psi_T \rangle|^2 \tag{67}$$

$$= \frac{\partial}{\partial B(k)_j} \langle \psi_d | \psi_T \rangle \langle \psi_T | \psi_d \rangle \tag{68}$$

$$= \left\langle \psi_d \middle| \frac{\partial \psi_T}{\partial B(k)_j} \right\rangle \langle \psi_T | \psi_d \rangle + \langle \psi_d | \psi_T \rangle \left\langle \frac{\partial \psi_T}{\partial B(k)_j} \middle| \psi_d \right\rangle \tag{69}$$

$$= 2\,\mathrm{Re}(\left\langle \psi_d \middle| \frac{\partial \psi_T}{\partial B(k)_j} \right\rangle \langle \psi_T | \psi_d \rangle) \tag{70}$$

$$= 2\,\mathrm{Re}(\left\langle \psi_d \middle| U_N \dots \frac{dU_j}{dB(k)_j} \dots U_1 \psi_0 \right\rangle \langle U_N \dots U_1 \psi_0 | \psi_d \rangle) \tag{71}$$

$$= 2\,\mathrm{Re}(\left\langle \psi_d \middle| -i\lambda_j \Delta t \frac{dH_j}{dB(k)_j} U_j \dots U_1 \psi_0 \right\rangle \langle \psi_T | \psi_d \rangle) \tag{72}$$

$$= 2\,\mathrm{Re}(\left\langle \psi_d \middle| -i\lambda_j \Delta t \frac{dH_j}{dB(k)_j} \psi_j \right\rangle \langle \psi_T | \psi_d \rangle) \tag{73}$$

$$= 2\,\mathrm{Re}(\langle \psi_d | -i\lambda_j \Delta t (H_{1,k} + 2B(k)_j H_{2,k}) \psi_j \rangle \langle \psi_T | \psi_d \rangle) \tag{74}$$

Here $\lambda_j = U_N \dots U_{j+1}$